



## OPEN LncRNA SNHG8 regulates the migration and angiogenesis of pHUVECs induced by high glucose via the TRPM7/ERK<sub>1/2</sub> signaling axis

Zongcheng Fan<sup>1,2,5</sup>, Xin Chen<sup>3,5</sup>, Laicheng Wang<sup>1,5</sup>, Jianjian Yu<sup>1</sup>, Shunpeng Zhang<sup>1</sup>, Changsheng Xu<sup>4</sup>, Jinxiu Lin<sup>3</sup>, Yunchai Lin<sup>3</sup>✉ & Feng Peng<sup>3</sup>✉

This study aimed to evaluate the regulatory effect and molecular mechanism of long noncoding RNA small nucleolus RNA host gene 8 (LncRNA SNHG8) in the migration and angiogenesis of primary human umbilical vein endothelial cells (pHUVECs) under high-glucose (HG) conditions. The HG-induced endothelial injury model was established in vitro. The cell model of silencing SNHG8, overexpressing SNHG8, and silencing TRPM7 was established by transfecting SNHG8-siRNA, SNHG8 plasmid and TRPM7-siRNA into cells with liposomes. The SNHG8 level was determined through reverse transcription-quantitative polymerase chain reaction (RT-qPCR). The expression levels of transient receptor potential melastatin 7 (TRPM7), endothelial nitric oxide synthase (eNOS), p-eNOS, extracellular signal-regulated kinase 1/2 (ERK1/2), and p-ERK1/2 were assessed through western blot. Nitric oxide (NO) levels were measured with DAF-FM. pHUVEC migration was examined through wound healing and Transwell assay, and pHUVEC angiogenesis was observed through a tube formation assay. Results showed that HG promoted the expression of LncRNA SNHG8 and TRPM7 and decreased the ratio of p-eNOS/eNOS and p-ERK<sub>1/2</sub>/ERK<sub>1/2</sub> in pHUVECs. NO production, migration, and angiogenesis were inhibited in pHUVECs under HG conditions. Silencing LncRNA SNHG8 and TRPM7 could significantly reverse the HG-induced decrease in eNOS activation, NO production, migration, and angiogenesis. SNHG8 and U0126 (ERK pathway inhibitor) overexpression enhanced the HG effects, whereas using U0126 did not affect the TRPM7 expression. In conclusion, LncRNA SNHG8 participates in HG-induced endothelial cell injury and likely regulates NO production, migration, and angiogenesis of pHUVECs via the TRPM7/ERK<sub>1/2</sub> signaling axis.

### Abbreviations

LncRNA	Long non-coding RNA
SNHG8	Small nucleolus RNA host gene 8
TRPM7	Transient receptor potential melastatin 7
pHUVEC	Primary human umbilical vein endothelial cell
ERK1/2	Extracellular regulated protein kinases1/2

Diabetes mellitus (DM) is one of the major global public health challenges<sup>1</sup>. Diabetic vascular disease is the leading cause of disability and premature mortality for patients with DM<sup>2</sup>. Injury and dysfunction of vascular endothelial cells (ECs), which are directly exposed to high glucose (HG), are major initiators of diabetic vascular disease<sup>3</sup>. Diabetic vascular disease exhibits impaired endothelium-dependent vasomotor effects and abnormal

<sup>1</sup>The First Clinical Medical College, Fujian Medical University, Fuzhou, Fujian, China. <sup>2</sup>Department of Cardiology, The Third People's Hospital of Hefei, Hefei, Anhui, China. <sup>3</sup>Department of Cardiology, National Regional Medical Center of Binhai Campus of the First Affiliated Hospital of Fujian Medical University, The First Affiliated Hospital of Fujian Medical University, Fuzhou, Fujian, China. <sup>4</sup>Fujian Provincial Institute of Hypertension, The First Affiliated Hospital of Fujian Medical University, Fuzhou, Fujian, China. <sup>5</sup>These authors contributed equally: Zongcheng Fan, Xin Chen and Laicheng Wang. ✉email: yunchailin@163.com; pengfeng@fjmu.edu.cn

survival, growth, and migration of ECs; among them, migration capability is critical for angiogenesis<sup>4</sup>. Therefore, endothelial dysfunction induced by hyperglycemia should be improved for the prevention and treatment of diabetic vascular disease.

Extracellular signal-regulated kinase 1/2 (ERK1/2) is a key mitogen-activated protein kinase. After being phosphorylated by various growth factors, hormones, and cytokines, ERK<sub>1/2</sub> can participate in meiosis, mitosis, and other functions, regulating cell growth, proliferation, differentiation, migration, and survival<sup>5,6</sup>. Nitric oxide (NO) is one of the proliferation-associated antiatherogenic vasoprotective factors. Phosphorylated endothelial nitric oxide synthase (eNOS) is the major source of NO production in ECs. ERK<sub>1/2</sub> can induce NO production in ECs via eNOS activation<sup>7</sup> and promote the proliferation, migration, and angiogenesis of human umbilical vein endothelial cells (HUVECs)<sup>8</sup>. Transient receptor potential melastatin 7 (TRPM7) is a membrane protein with kinase and ion channel function; when activated by HG, shear stress, oxidative stress, and other stimulations, it can impair EC function by inhibiting the ERK1/2 pathway<sup>9,10</sup>. Silencing TRPM7 can increase phosphorylated ERK1/2, upregulate the expression of eNOS and NO, and promote endothelium-dependent vasomotor effects<sup>11</sup>. In addition, TRPM7 protein level was increased in high-glucose treated cells and diabetic mice, which reduced NOS level and increased apoptosis, inducing cell damage<sup>12</sup>.

Long noncoding RNAs (lncRNAs) are RNA transcripts with a length of over 200 nucleotide units without protein-coding functions<sup>13</sup>; they participate in the initiation and development of atherosclerosis<sup>14</sup>. Small nucleolar RNA host gene 8 (SNHG8), a novel small nucleolar RNA located at 4q26, is involved in multiple biological functions, such as translation, transcription, RNA splicing, transcription regulation, and signal transduction<sup>15</sup>. Tao et al. demonstrated that SNHG8 promotes the proliferation, migration, invasion, and metastasis of gastric cancer, and the upregulation of SNHG8 expression in gastric cancer morbidity increases<sup>16</sup>. SNHG8 can inhibit human islet  $\beta$ -cell proliferation, reduce insulin levels, and increase blood glucose levels through nucleosome assembly protein 1-like 1 (NAP1L1) to inhibit the transcription of p57 (Kip2)<sup>17,18</sup>. Our previous FIESTA study also suggested that lncRNA SNHG8 is highly expressed in patients with increased fasting glucose<sup>19</sup>. Huang et al. showed that lncRNA SNHG8 interacts with Epstein–Barr virus proteins LF3, BHLF1, BHRF1, and BNLF2a through co-expression and enrichment analysis. These proteins in turn regulate the expression of TRPM7, TRIM28, EIF4A2, NAP1L1, PLD3, and RPL18A<sup>16</sup>. It suggests an indirect regulatory relationship between lncRNA SNHG8 and TRPM7. However, the role of the SNHG8/TRPM7 pathway in diabetic vascular EC dysfunction remains unknown.

On the basis of these findings, we conducted this study to investigate the effects of lncRNA SNHG8 on the NO production, migration, and angiogenesis of HG-induced HUVECs and determine whether lncRNA SNHG8 could promote TRPM7 expression and then inhibit ERK1/2 pathway activation to cause endothelial dysfunction. These results provided a theoretical basis for screening new antidiabetic angiopathy drug targets.

## Methods and materials

### Cell culture and identification

Primary human umbilical vein endothelial cells (pHUVECs) were isolated from a neonatal umbilical cord through type I collagenase digestion method<sup>20</sup>. They were cultured in ECM (Cat. no. 001; ScienCell, USA) medium containing 5% FBS, 0.1% ECG, 100 U/mL penicillin, and 100  $\mu$ g/mL streptomycin and incubated in 5% CO<sub>2</sub> at 37 °C. The ECs presented a paving stone-like pattern under a microscope. Immunofluorescence Factor VIII (Cat. no. AM-0022; ZSGB, China) and CD31 (Cat. no. A4900; ABclonal, China) antibodies for identification were positive in pHUVECs. Cell identification results are shown in supplementary material. Studies were only performed with cells at passages 3–6. The study was approved by The Animal Medical Ethics Committee of Fujian Medical University (research license number: FJMU IACUC 2022-NSFC-0376). Informed signed consent was obtained from all subjects involved in the study. All experiments and methods were performed in accordance with relevant guidelines and regulations.

### Cell transfection

An SNHG8-expressing plasmid (pCDNA3.1 vector) and siRNAs targeting SNHG8 (si-SNHG8), TRPM7 (si-TRPM7), negative control (si-NC) were assembled by Hanheng Biotechnology (Shanghai, China). pHUVECs were transfected using LipoFiter 3.0 (Hanheng, China) in accordance with the manufacturer's instructions. The cells were treated with 30 mM D-glucose (Cat. no. G7021; Sigma, USA) for 72 h and 10<sup>-5</sup> M U0126 (Cat. no. S1901; Beyotime, China)<sup>21</sup> for 30 min.

### Reverse transcription-quantitative PCR (RT-qPCR)

According to the manufacturer's instructions, RNA was extracted with TRIZOL reagent (Cat. no. ER501-01; Transgen, China) and reversely transcribed into cDNA templates by using a reverse transcription kit (Cat. no. 11141ES60; Yeasen, China). SYBR Green master mix (Cat. no. 11202ES03; Yeasen, China) was used for qPCR amplification. Relative quantification was performed using the 2<sup>- $\Delta\Delta$ Ct</sup> method and normalized to  $\beta$ -actin<sup>22</sup>. The following primer sequences were used:  $\beta$ -actin, forward 5'-GCATGGAGTCCTGTCGCATCC-3' and reverse 5'-GCGGCCAGGATGGAGCCGC-3'; SNHG8, forward 5'-GCTGAGCTGAACACATTACG-3' and reverse 5'-ACGATAAGTCCATTGCCGGA-3'.

### Western blot analysis

Western blot was performed as previously reported<sup>23</sup>. The total protein from the cells was extracted using RIPA lysed buffer (Cat. no. P0013B; Beyotime, China), and its quality was determined using a BCA kit (Cat. no. P0012S; Beyotime, China). Proteins were loaded onto 4%–20% SDS-PAGE (Cat. no. F11420Gel; ACE, China) and transferred to PVDF membranes (Cat. no. IPVH00010; Merck Millipore, Germany). According to the

molecular weight of the protein, the reference and target proteins were cut separately at the corresponding positions of the membrane. The membranes were then exposed to 5% skim milk and probed with primary antibodies against TRPM7 (1:1000; ab262698; Abcam), eNOS (1:1000; abB252439; Abcam), phosphorylation-eNOS (1:1000; ab215717; Abcam), ERK1/2 (1:1000; ab184699; Abcam), phosphorylation-ERK1/2 (1:1000; ab278538; Abcam), and  $\beta$ -actin antibody (1:10,000; AC026; ABclonal) at 4 °C overnight. They were incubated with secondary antibodies HRP-goat anti-rabbit (1:10,000; AS014; ABclonal) at room temperature for 1 h. Protein bands were detected on a chemiluminescence system by using an ECL kit (Cat. no. P10100; NCM, China).

### NO measurements

After cell transfection and high glucose treatment, each six-well plate was added with 1 ml of DAF-FM DA (dilution 1:1000; Beyotime, China) with a final concentration of 5  $\mu$ mol/l. The sample was incubated for 20 min and washed thrice with phosphate-buffered saline (PBS). Cells were randomly selected for visualization and photographed under a fluorescence microscope Objective lens 100 $\times$  (Olympus, Japan). Immunofluorescence staining was quantitatively assessed with ImageJ 1.6.

### Wound healing assay

After cell transfection and high glucose treatment, pHUVECs were planted equally into a six-well plate and cultured to 80–90% confluent. Then, the cells were incubated in the medium with 1% FBS, and vertical scratches were drawn by a 200  $\mu$ L pipette tip. The cells were photographed by Inverted microscopy OLYMPUS DP71/72 (Objective lens 100 $\times$ ) at 0, 24 h after scraping. Wound healing percentage was used to evaluate migratory abilities of pHUVECs. Wound healing percentage =  $[(A - B)/A] \times 100\%$ , where A is the average wound surface area at 0 h and B is the average wound surface area at 24 h. Wound surface area was measured by ImageJ.

### Cell migration assay

Transwell chambers (Cat. no. 3422; Corning, USA) were used for cell migration assays. In this procedure, 200  $\mu$ l of pHUVEC suspension at a density of  $1 \times 10^5$ /chamber were added to the serum-free medium in the upper chamber, and the relevant medium containing 10% FBS was added to the lower chamber as a chemoattractant. After being incubated for 24 h, the cells in the upper chamber were removed using cotton swabs, while the cells in the lower chamber were fixed with formaldehyde and stained with 0.1% crystal violet staining solution (Cat. no. C0121; Beyotime, China) for 20 min. They were then imaged under a microscope (Objective lens 200 $\times$ ). The number of migrated cells was calculated using ImageJ.

Tube formation assay. Matrigel (Cat. no. 356234; Corning, USA), 48-well culture plates, and pipette tips were exposed to 4 °C overnight. After being precooled, the Matrigel was spread in 48-well plates and cured in incubators at 37 °C for 30 min. Then, 200  $\mu$ l of pHUVEC suspension ( $1.5 \times 10^5$  PCS/ml) was added to the Matrigel surface and incubated at 37 °C for 4–6 h. Then, the Matrigel was imaged under a microscope (Objective lens 100 $\times$ ) to quantify tube formation for each plate and analyzed using ImageJ.

### Statistical analysis

The procedures were repeated thrice. Quantitative data were evaluated using GraphPad Prism 8 (GraphPad Software Inc., San Diego, CA, USA). All experimental data were quantitative data and presented as means  $\pm$  SEs. Student's t-test was conducted to compare the difference between two groups, and one-way ANOVA was conducted for multiple groups. Pairwise comparisons between groups were applied through the least significant difference (LSD) method. Results were statistically significant when  $P < 0.05$ .

## Results

### HG promoted the lncRNA SNHG8 expression in pHUVECs

To investigate the effect of SNHG8 on ECs under HG condition, we detected the SNHG8 expression after the cells were exposed to 5.5 mM glucose (CTL group) to 33 mM glucose for 72 h and to 30 mM glucose for 0 h (CTL group) to 96 h. We used mannitol as an osmolality control. We found that as the glucose concentration increased, the SNHG8 expression showed a concentration-dependent induction of expression ( $P < 0.01$ , Fig. 1A). SNHG8 did not differ between HG 30 mM and HG 33 mM groups ( $P > 0.05$ , Fig. 1A). HG 72 and 96 h groups significantly enhanced the SNHG8 expression ( $P < 0.01$ , Fig. 1B). SNHG8 did not differ between HG72 h and HG96 h groups, and CTL and mannitol groups, ( $P > 0.05$ , Fig. 1B, C).

### HG downregulated the eNOS activation and NO production of pHUVECs via SNHG8

The cells were transfected with siRNA against SNHG8, scrambled siRNA (siRNA NC), or lipofectamine alone and cultured with 30 mM glucose for 72 h. The expression efficiency of SNHG8 was detected through RT-qPCR. The results showed that the SNHG8 expression in the HG + si-SNHG8 group was significantly lower than that in the HG group, and the transfection efficiency was  $> 70\%$  ( $P < 0.01$ , Fig. 2A). No significant difference was found between HG and HG + Si-NC groups ( $P > 0.05$ , Fig. 2A). The cells were transfected with SNHG8 plasmid, Empty plasmid vector (CTL plasmid), and cultured with 30 mM glucose for 72 h. The expression efficiency of SNHG8 was detected through RT-qPCR. The results showed that the SNHG8 expression in the HG + SNHG8 plasmid group was significantly higher than that in the HG group, and the overexpression efficiency was  $> 300\%$  ( $P < 0.01$ , Fig. 2B). No significant difference was found between HG and HG + control plasmid groups ( $P > 0.05$ , Fig. 2B).

Furthermore, we conducted Western blot to evaluate eNOS and p-eNOS expression and used the fluorescent probe DAF-FM DA to assay the NO production. Western blot and DAF-FM DA assay showed that HG significantly reduced the ratio between p-eNOS and total eNOS ( $P < 0.05$ , Fig. 2C, D) and downregulated NO

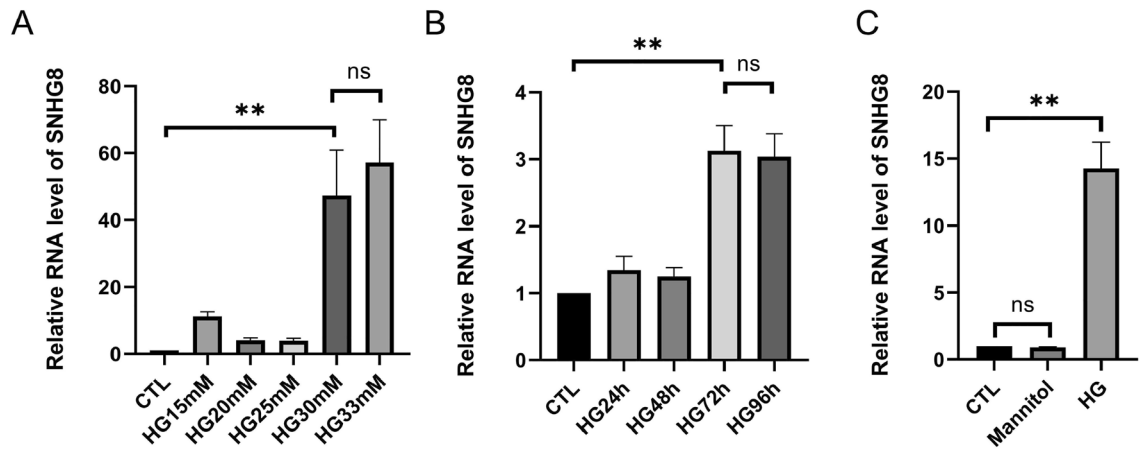


**Figure 1.** HG treatment promotes lncRNA SNHG8 expression in pHUVECs. (A) pHUVECs were stimulated with 5.5 mM glucose (CTL), 15 mM, 20 mM, 25 mM and 33 mM glucose (HG) for 72 h. (B) pHUVECs were stimulated with HG (30 mM) for 24, 48, 72, and 96 h. (C) pHUVECs were stimulated with HG (30 mM) and Mannitol (30 mM) for 72 h. The level of lncRNA SNHG8 was detected by RT-qPCR. (\*\*,  $P < 0.01$ ; ns,  $P > 0.05$ ;  $n = 3$ ).

production ( $P < 0.001$ , Fig. 2E, F). SNHG8 further reduced p-eNOS and NO production ( $P < 0.01$ , Fig. 2C–F). Si-SNHG8 significantly reversed these trends ( $P < 0.05$  and  $P < 0.001$ , Fig. 2C–F). The p-eNOS/eNOS ratio and NO production did not significantly differ between the CTL and mannitol groups, the HG and HG + si-NC groups, and the HG and HG + control plasmid groups ( $P > 0.05$ , Fig. 2C–F). Therefore, HG stimulated lncRNA SNHG8 to regulate the eNOS activation and NO production of pHUVECs.

#### SNHG8 regulated the migration and angiogenesis of HG-induced pHUVECs

In Fig. 3, wound healing and Transwell assay were used to evaluate the effect of the migratory abilities of pHUVECs, and the tube formation assay on Matrigel were used to assess the angiogenic capability. The migratory ability ( $P < 0.001$ , Fig. 3A–D) and angiogenic ability ( $P < 0.01$ , Fig. 3E, F) of pHUVECs were reduced under HG conditions compared to control group. SNHG8 siRNA significantly reversed these trends ( $P < 0.001$ , Fig. 3A–D and  $P < 0.01$ , Fig. 3E, F). Migration and angiogenesis could be further suppressed by SNHG8 plasmid ( $P < 0.05$ , Fig. 3A–F). The migratory and angiogenic capability did not significantly differ between the CTL and mannitol groups, the HG and HG + si-NC groups, and the HG and HG + control plasmid groups ( $P > 0.05$ , Fig. 3A–F). Therefore, lncRNA SNHG8 could regulate the migration and angiogenesis of HG-induced pHUVECs.

#### SNHG8 regulated the TRPM7/ERK1/2 pathway of pHUVECs under HG condition

To investigate the possible regulatory relationship between the lncRNA SNHG8 and TRPM7/ERK<sub>1/2</sub> pathway, we conducted Western blot to determine the expression of TRPM7, ERK<sub>1/2</sub>, p-ERK<sub>1/2</sub> after SNHG8 was silenced and overexpressed. HG significantly increased the TRPM7 expression ( $P < 0.05$ , Fig. 4A, B) and decreased the ERK<sub>1/2</sub> activation ( $P < 0.01$ , Fig. 4A, C). Si-SNHG8 significantly decreased the TRPM7 expression ( $P < 0.01$ , Fig. 5A, B) and increased the ERK<sub>1/2</sub> activation ( $P < 0.01$ , Fig. 4A, C). While SNHG8 plasmid further increased the TRPM7 expression ( $P < 0.05$ , Fig. 4A, B) and decreased the ERK<sub>1/2</sub> activation ( $P < 0.01$ , Fig. 4A, C). No significant differences in the TRPM7 expression and decreased ERK<sub>1/2</sub> activation were found between the CTL and mannitol groups, the HG and HG + si-NC groups, and the HG and HG + control plasmid groups ( $P > 0.05$ , Fig. 4A–C).

To further confirm the regulatory relationship between TRPM7 and ERK<sub>1/2</sub>, we transfected si-TRPM7 through lipofection to silence TRPM7 and used U0126 (ERK pathway inhibitor) to inhibit ERK<sub>1/2</sub> activation under HG conditions. Western blot results indicated that si-TRPM7 significantly increased ERK<sub>1/2</sub> activation ( $P < 0.05$ , Fig. 4D, F). U0126 significantly reduced ERK<sub>1/2</sub> activation, whereas no significant deviation was found in the TRPM7 expression ( $P > 0.05$ , Fig. 4D, E). TRPM7 expression and ERK<sub>1/2</sub> activation did not significantly differ between the HG and HG + si-NC groups ( $P > 0.05$ , Fig. 4D–F). These results suggested that lncRNA SNHG8 involved in regulating the TRPM7 expression and ERK<sub>1/2</sub> activation of HG-induced pHUVECs. TRPM7 is an upstream molecule that regulates ERK<sub>1/2</sub> activation.

#### TRPM7/ERK1/2 pathway regulated the eNOS activation and NO production of pHUVECs under HG condition

In Fig. 5, we conducted Western blot and fluorescent probe DAF-FM DA test after TRPM7 was silenced and ERK<sub>1/2</sub> activation was inhibited. Si-TRPM7 significantly increased the p-eNOS/eNOS ratio and NO production under HG ( $P < 0.01$ , Fig. 5A, B;  $P < 0.001$ , Fig. 5C, D). U0126 significantly decreased the p-eNOS/eNOS ratio and NO production under HG ( $P < 0.01$ , Fig. 5A–D). The p-eNOS/eNOS ratio and NO production had no significant differences between the HG and HG + si-NC groups ( $P > 0.05$ , Fig. 5A–D). These results suggested that the TRPM7/ERK1/2 pathway involved in eNOS activation and NO production regulation of pHUVECs.

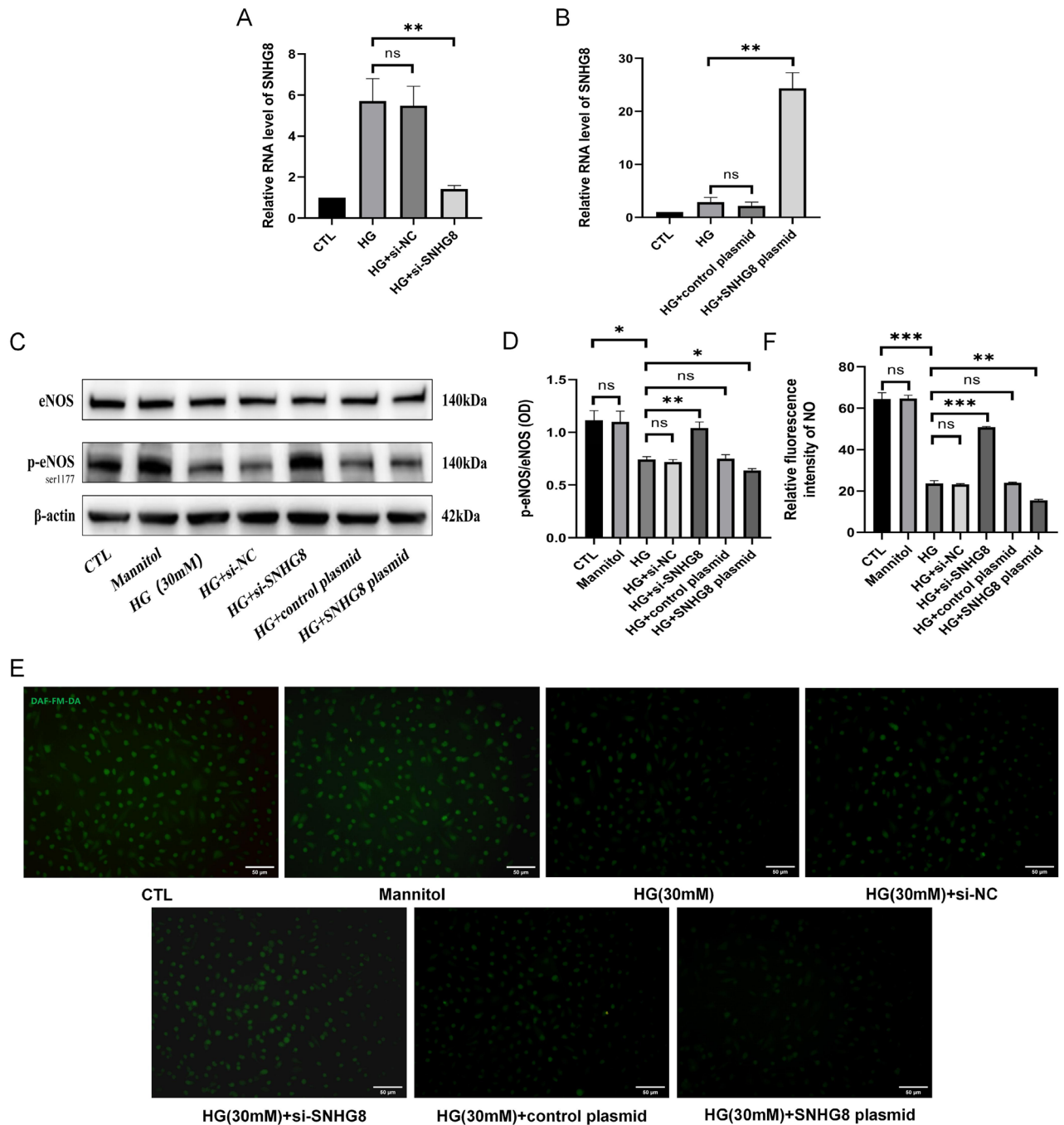


**Figure 2.** LncRNA SNHG8 regulated eNOS activity and NO production in HG-stimulated pHUVECs. pHUVECs were transfected with SNHG8 siRNA and SNHG8 pcDNA3.1 plasmid by LipoFiter3.0 transfection for 6 h; the culture medium was changed (negative control group was set) and stimulated with HG (30 mM) for 72 h. (A) siRNA-SNHG8 was transfected into pHUVECs. (B) SNHG8 plasmids were transfected into pHUVECs. (C) Western blot analysis of the eNOS and p-eNOS expression levels in pHUVECs. (D) Quantitative analysis of eNOS activity, denoted by p-eNOS/eNOS (OD) ratio. (E) DAF-FM-DA fluorescent probe was used to detect NO production in pHUVECs (scale = 50  $\mu$ m). (F) Quantitative analysis of NO production, denoted by green fluorescence intensity. The level of lncRNA SNHG8 was detected through RT-qPCR (\*,  $P < 0.05$ ; \*\*,  $P < 0.01$ ; \*\*\*,  $P < 0.001$ , ns,  $P > 0.05$ ;  $n = 3$ ).

induced by HG. These results suggested that the TRPM7/ERK1/2 pathway involved in the eNOS activation and NO production regulation of pHUVECs induced by HG.

### TRPM7/ERK1/2 pathway regulated the migration and angiogenesis of pHUVECs under HG

In Fig. 6, we conducted the scratch test, the Transwell assay, and the tube formation assay after TRPM7 was silenced and ERK<sub>1/2</sub> activation was inhibited. The wound healing rate ( $P < 0.001$ , Fig. 6A, B), migration abilities

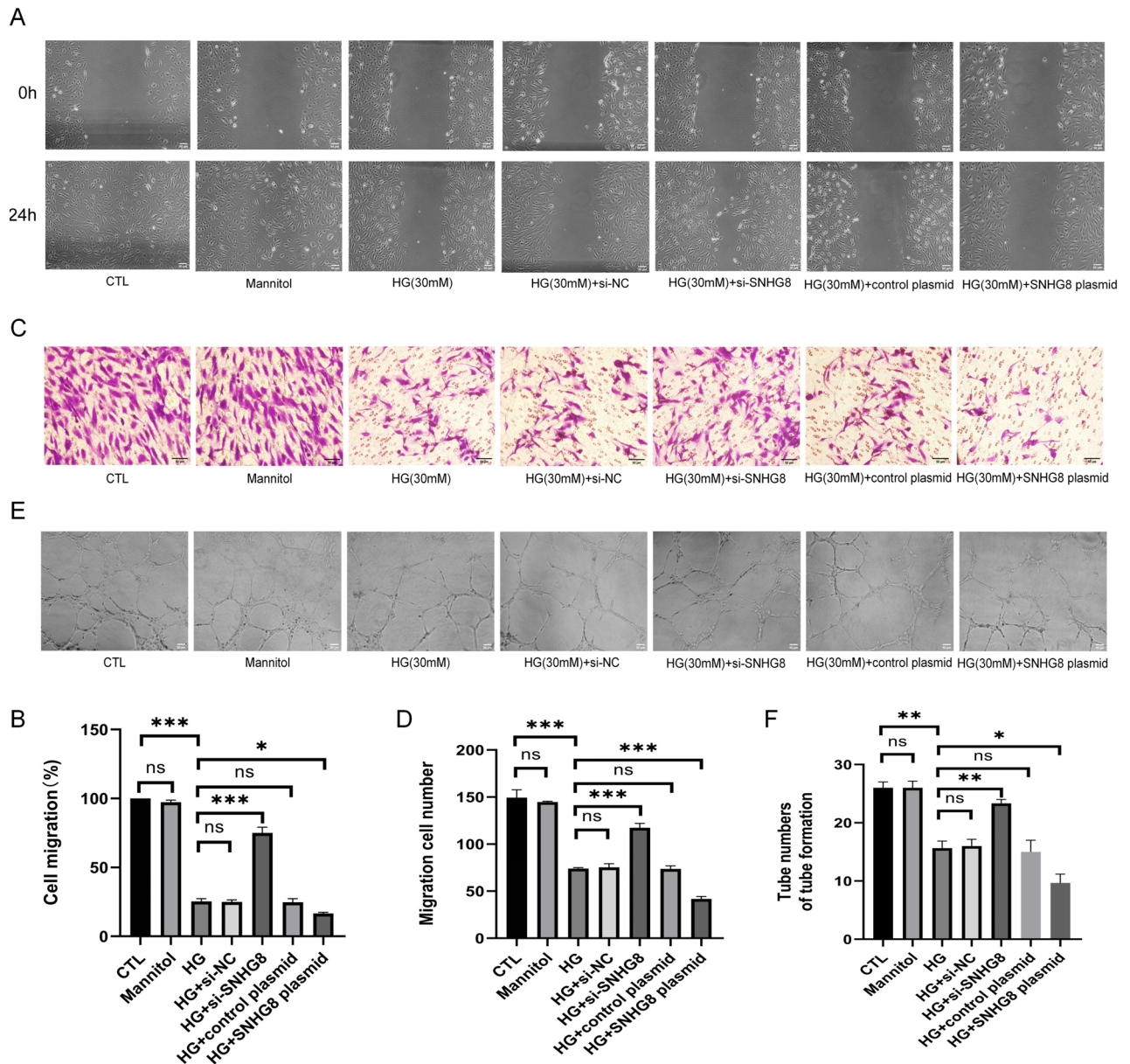


**Figure 3.** LncRNA SNHG8 regulated the migration and angiogenesis of pHUVECs under HG stimulation. pHUVECs were transfected with SNHG8 siRNA and SNHG8 pcDNA3.1 plasmid through LipoFiter3.0 transfection for 6 h. The culture medium was changed (negative control group was set up) and stimulated with HG (30 mM) for 72 h. (A) pHUVEC migration was detected through a scratch test (scale = 50  $\mu$ m). (B) Quantitative analysis of the scratch test; the migration level of pHUVECs was expressed as the healing rate. (C) pHUVEC migration was detected through a Transwell assay (scale = 50  $\mu$ m). (D) Quantitative analysis of the Transwell assay by using the number of the transplanted cells to represent the migration level of pHUVECs. (E) pHUVEC angiogenesis was detected using a tube formation test (scale = 50  $\mu$ m). (F) Quantitative analysis of the tube formation test; the number of tubes of pHUVECs as the angiogenesis level expression (\*,  $P < 0.05$ ; \*\*,  $P < 0.01$ ; \*\*\*,  $P < 0.001$ , ns,  $P > 0.05$ ;  $N = 3$ ).

( $P < 0.05$ , Fig. 6C, D), and angiogenesis ( $P < 0.01$ , Fig. 6E, F) of the HG + Si-TRPM7 group significantly increased compared with that of the HG group. Conversely, U0126 significantly decreased the wound healing rate, migration abilities, and angiogenesis ( $P < 0.01$ , Fig. 6A–F). Migratory abilities and angiogenic capability had no significant differences between the HG and HG + si-NC groups ( $P > 0.05$ , Fig. 6A–F). These results suggested that the TRPM7/ERK<sub>1/2</sub> pathway regulated the migration and angiogenesis of pHUVECs under HG condition.

## Discussion

The impairment of endothelium-dependent vessel relaxation and the dysregulation of angiogenesis are the main causes of vascular complications in diabetes<sup>24</sup>. Increased blood glucose levels induce the mitochondria to produce excessive ROS through the protein kinase C (PKC) pathway. Then, excessive ROS downregulates bioavailable

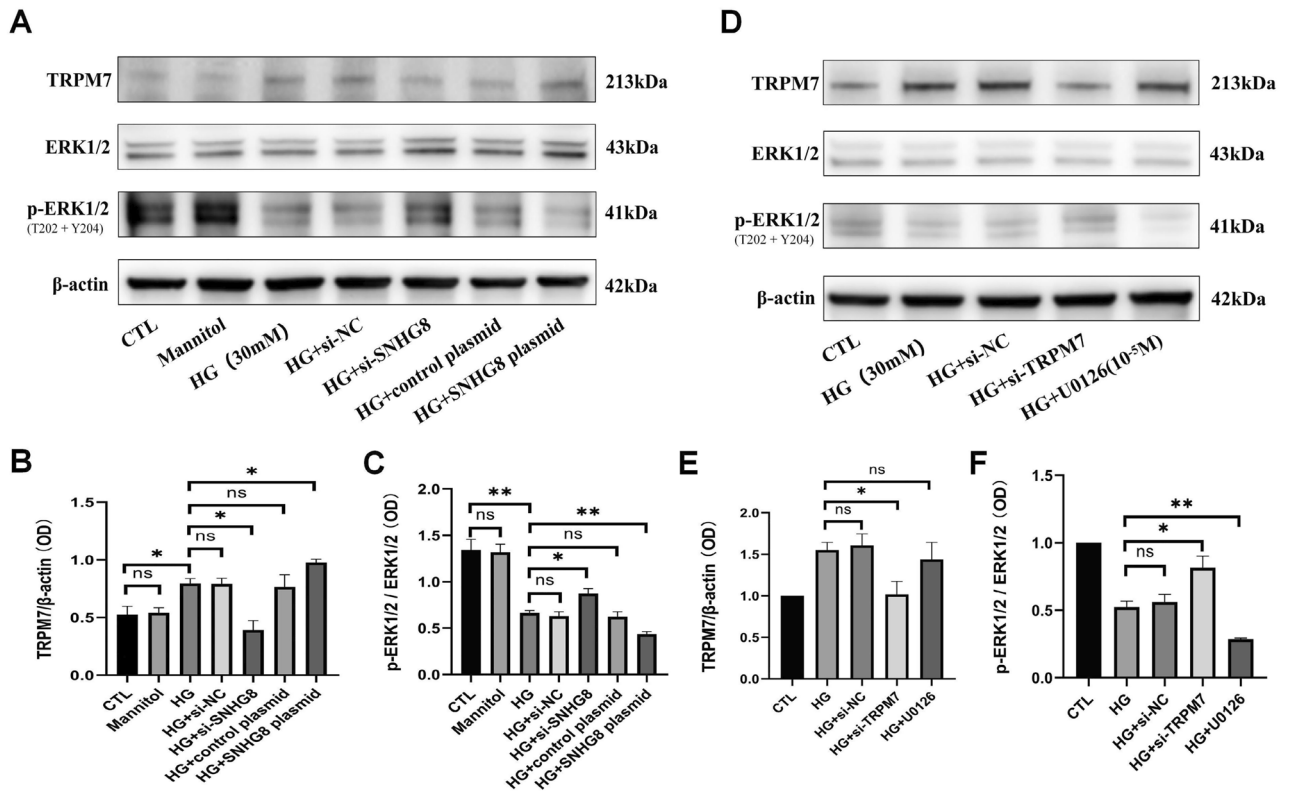


**Figure 4.** LncRNA SNHG8 regulated the TRPM7/ERK<sub>1/2</sub> signaling pathway in HG-stimulated pHUVECs. pHUVECs were transfected with SNHG8 siRNA and SNHG8 pcDNA3.1 plasmid by LipoFiter3.0 for 6 h. The culture medium was changed (negative control group was set up) and stimulated with HG (30 mM) for 72 h. (A) Western blot analysis of TRPM7, ERK1/2, and p-ERK1/2 expression levels in pHUVECs. (B) Quantitative analysis of TRPM7 expression levels. (C) Quantitative analysis of ERK1/2 activity, denoted by the p-ERK<sub>1/2</sub>/ERK<sub>1/2</sub> (OD) ratio. Subsequently, pHUVECs were transfected with TRPM7 siRNA by LipoFiter3.0 for 6 h. The culture medium was changed (negative control group was set up), and HG (30 mM) was added for 72 h, 10<sup>-5</sup> M U0126 (ERK pathway inhibitor) for 30 min. (D) Western blot analysis of TRPM7, ERK1/2, and p-ERK1/2 expression. (E) Quantitative analysis of TRPM7 expression. (F) Quantitative analysis of ERK1/2 activity, denoted by the p-ERK<sub>1/2</sub>/ERK<sub>1/2</sub> (OD) ratio. (\*, P < 0.05; \*\*, P < 0.01; Ns, P > 0.05; N = 3).

NO levels by reducing the eNOS activity and leads to impaired vasorelaxation<sup>25</sup>. Angiogenesis plays an essential role in atherosclerosis<sup>26</sup>. Angiogenesis begins with vascular germination, and vascular endothelial growth factor (VEGF) binds to vascular endothelial growth factor receptor 2 (VEGFR2) expressed by ECs. VEGFR2 activation induces numerous signaling cascades that promote angiogenesis<sup>27,28</sup>. HG induces ECs to promote VEGFR2 phosphorylation and inhibit the binding to VEGF, thereby inhibiting angiogenesis<sup>29</sup>. In this study, pHUVECs were obtained from the umbilical cords of healthy newborns and used as model ECs. A pHUVEC HG-induced injury model was established, revealing that HG impaired the eNOS activity, NO production, migration, and angiogenesis ability of ECs. LncRNA SNHG8 was highly expressed under HG conditions. Moreover, silencing SNHG8 could retrieve HG-induced impairment of ECs, and SNHG8 overexpression could further stress the impairment. These results were consistent with the theory that HG promoted vascular endothelial vasodilatory and angiogenesis dysfunction.

LncRNAs are important gene expression and pathogenesis regulatory factors<sup>30</sup>, which serve as signals, bait, guide, or scaffold molecules by binding to proteins, DNAs, RNAs, and their combinations<sup>31</sup>. Former studies have mainly focused on their function as proliferation, migration, invasion promotor, and apoptosis inhibitor in tumors such as gastric cancer, breast cancer, and colorectal cancer<sup>32</sup>. Yu et al. suggested that SNHG8 promotes breast cancer cell proliferation, migration, and invasion through the miR-634/ZBTB20 pathway<sup>33</sup>. Likewise, Tian et al. indicated that SNHG8 participates in diffuse large B cell lymphoma cell proliferation and colony formation, thereby inhibiting cell apoptosis<sup>34</sup>. LncRNA SNHG8 also regulates non-neoplastic diseases. In a myocardial infarction model, SNHG8 can modulate the NF-κB signaling pathway to inhibit cell viability

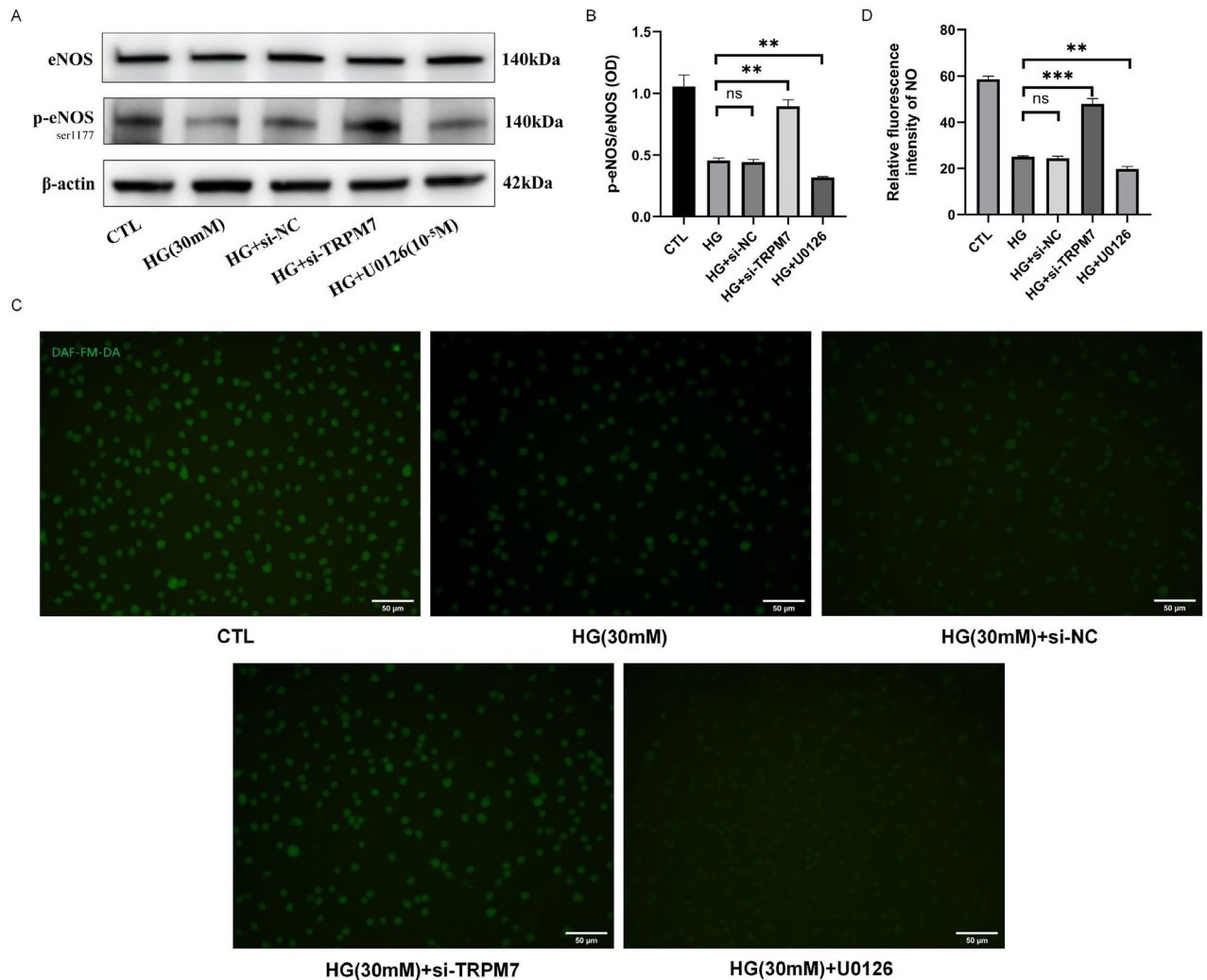


**Figure 5.** TRPM7/ERK<sub>1/2</sub> signaling pathway regulated the eNOS activity and NO production of pHUVECs stimulated by HG. pHUVECs were transfected with SNHG8 siRNA and SNHG8 pcDNA3.1 plasmid by LipoFiter3.0 transfection for 6 h. The culture medium was changed (negative control group was set up) and stimulated with HG (30 mM) for 72 h. (A) Western blot analysis of eNOS and p-eNOS expression levels in pHUVECs. (B) Quantitative analysis of eNOS activity, denoted by p-eNOS/eNOS (OD) ratio. (C) DAF-FM-DA fluorescent probe was used to detect NO production in pHUVECs (scale = 50 μm). (D) Quantitative analysis of NO production, denoted by green fluorescence intensity. (\*\*,  $P < 0.01$ ; \*\*\*,  $P < 0.001$ , ns,  $P > 0.05$ ;  $n = 3$ ).

and induce apoptosis<sup>35</sup>. It can promote inflammatory reactions in the microvascular ECs of a mouse brain<sup>36</sup>. However, no functional studies about lncRNA SNHG8 in HUVECs impaired by HG have been performed. Our study suggested that SNHG8 was highly expressed in HG-induced pHUVECs, which was consistent with the results of our FIESTA study<sup>19</sup>. LncRNA SNHG8 initially increased, decreased, and increased further as the glucose concentration increased. Because no relevant articles on the SNHG8 expression under different glucose concentrations have been published, we cannot fully explain this phenomenon at present. A previous report in China showed that as the glucose concentration increased, cell proliferation and viability can be initially promoted and subsequently inhibited. This phenomenon may be caused by the effect of glucose on the energy metabolism, transcription, and secretion of cytokines of ECs, but it should be further investigated in the future. Furthermore, our results demonstrated that SNHG8 exerted inhibitory effects on migration and angiogenesis, which were different from tumor cell models. This heterogeneity relies on the characteristics of HG-induced pHUVECs, which are significantly different from cancer cells and the tumor microenvironment. Therefore, silencing SNHG8 expression could improve vascular endothelial function, which might provide a new strategy for preventing diabetic vascular disease.

TRPM7 is an important function molecule in HUVECs<sup>37</sup>. Its expression increases in HUVECs cultured with low serum magnesium levels, and silencing TRPM7 expression can promote HUVEC migration and angiogenesis<sup>9</sup>. Sun et al. suggested that downregulated TRPM7 expression in HUVECs stimulated by HG can decrease ROS generation and eNOS expression; it can also increase cell viability to improve HG-induced vascular EC damage<sup>38</sup>. TRPM7 is involved in the angiogenesis of ECs<sup>39</sup>. MiR-9-5p through the PI3K/AKT/autophagy pathway targeting TRPM7 to promote the proliferation, migration, and angiogenesis of ECs<sup>40</sup>. TRPM7 kinase is



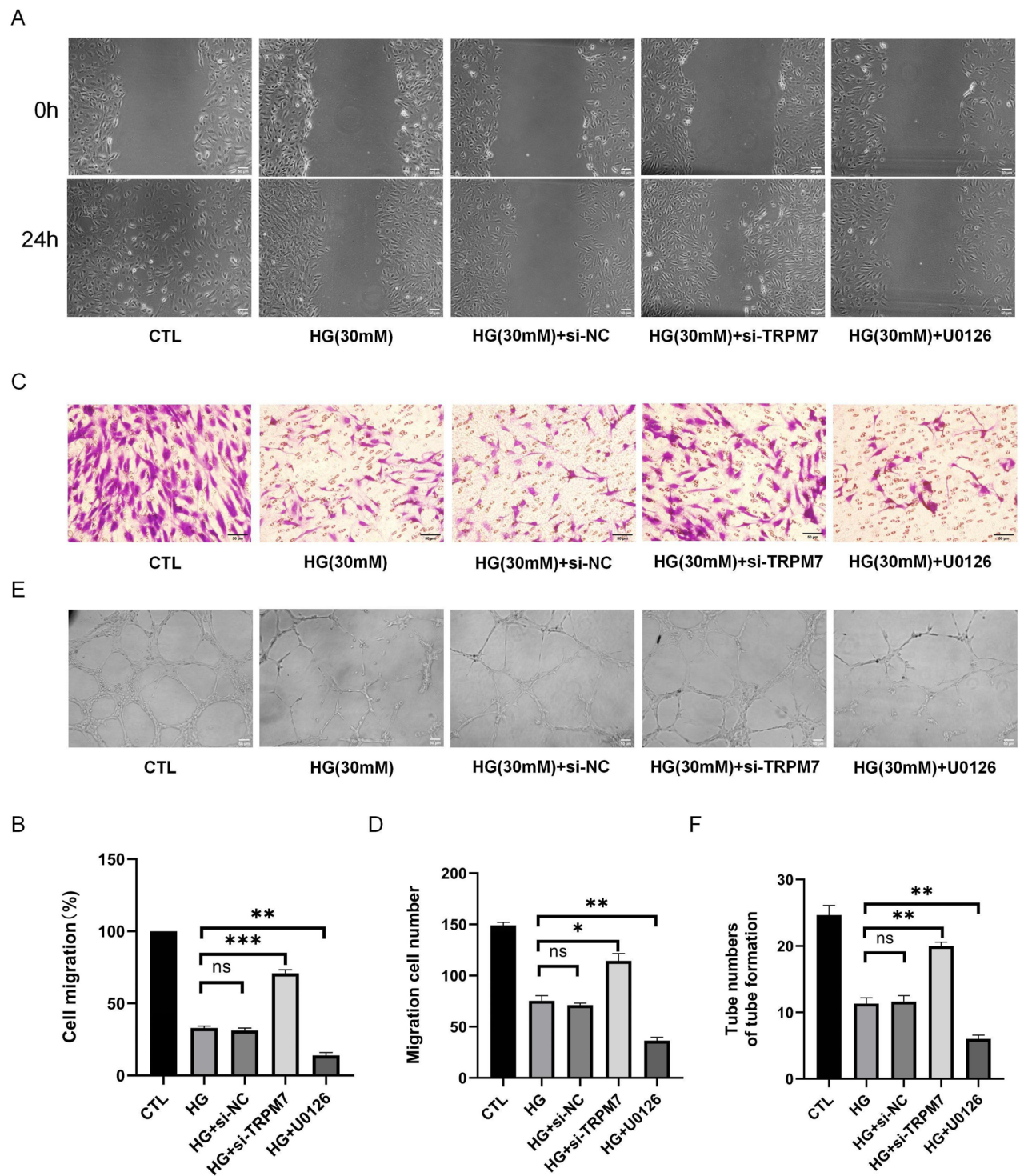


**Figure 6.** TRPM7/ERK<sub>1/2</sub> signaling pathway regulates the migration and angiogenesis of pHUVECs under HG stimulation. pHUVECs were transfected with TRPM7 siRNA and treated with 10<sup>-5</sup> M U0126 followed by HG (30 mM) stimulation for 72 h. (A) pHUVEC migration was detected via a scratch test (scale = 50 μm). (B) Quantitative analysis of the scratch test; the migration level of pHUVECs was expressed as the healing rate. (C) pHUVEC migration was detected via a Transwell assay (scale = 50 μm). (D) Quantitative analysis of the Transwell assay involving the number of transplanted cells to represent the migration level of pHUVECs. (E) Angiogenesis of pHUVECs was detected through a tube formation test (scale = 50 μm). (F) Quantitative analysis of the tube formation test; the number of tubes of pHUVECs as the expression of angiogenesis level (\*, P < 0.05; \*\*, P < 0.01; \*\*\*, P < 0.001, ns, P > 0.05; N = 3).

also a regulator of insulin synthesis,  $\beta$ -cell dynamics, and glucose homeostasis. TRPM7 reduces insulin secretion of  $\beta$ -cells by inhibiting AKT/ERK signaling pathway<sup>41</sup>. In addition, high glucose significantly increased NF- $\kappa$ B activity and ROS production in HUVECs<sup>42</sup>, and high glucose also promoted the upregulation of TRPM7 expression, which activated the transcription of NF- $\kappa$ B<sup>43</sup>. Recently, it has been found that high glucose induces the demethylation of NF- $\kappa$ B promoter region, which leads to the increase of its mRNA expression<sup>44</sup>. Therefore, the interaction between TRPM7 and NF- $\kappa$ B in high glucose conditions was not further explored in this study.

The Ras/Raf/MEK/ERK signaling pathway is closely correlated with the proliferation, migration, and angiogenesis of ECs. When Ras and GTP are combined in an activated state, Raf can be activated, and MEK1/2 can be further activated. Activated MEK1/2 releases ERK1/2 (T202/Y204), and activated ERK1/2 can be transferred to the nucleus and regulate cell proliferation, migration, and differentiation by regulating the transcription factor activity<sup>45</sup>. For example, miR-155 downregulates ERK1/2 activation to reduce HUVEC damage and apoptosis and promotes HUVEC migration and capillary formation<sup>46</sup>. Silencing TRPM7 can promote ERK1/2 activation and myosin light chain (MLC) phosphorylation, attenuate HUVEC adhesion to the matrix, and promote cell migration, wound healing, and angiogenesis processes<sup>10</sup>. In this study, TRPM7 was highly expressed, and the p-ERK1/2 expression was downregulated under the HG condition through Western blot assay. Furthermore, TRPM7 expression was downregulated by silencing lncRNA SNHG8 under HG, while p-ERK1/2 expression was upregulated, thereby improving the NO production, migration, and angiogenesis of pHUVECs; however, SNHG8 overexpression reversed this appeal. We found that silencing TRPM7 under HG condition could increase the ERK1/2 activity, improved the eNOS activity, migration, and angiogenesis ability of pHUVECs, while using U0126 (ERK pathway inhibitor) reversed these results, but did not affect the TRPM7 expression. These results suggested that the SNHG8/TRPM7/ERK<sub>1/2</sub> signaling axis might regulate HG-induced EC injury.

## Conclusion

LncRNA SNHG8 plays an important role in HG-induced endothelial cell injury and may regulate the NO production, migration, and angiogenesis of pHUVECs via the TRPM7/ERK<sub>1/2</sub> signaling axis (Fig. 7). While previous studies on lncRNA SNHG8 mainly focused on cancer, this study is the first to investigate the regulatory role of SNHG8 in a HG-induced pHUVEC injury model and provide a theoretical basis for determining and screening new therapeutic targets for diabetic vascular disease.

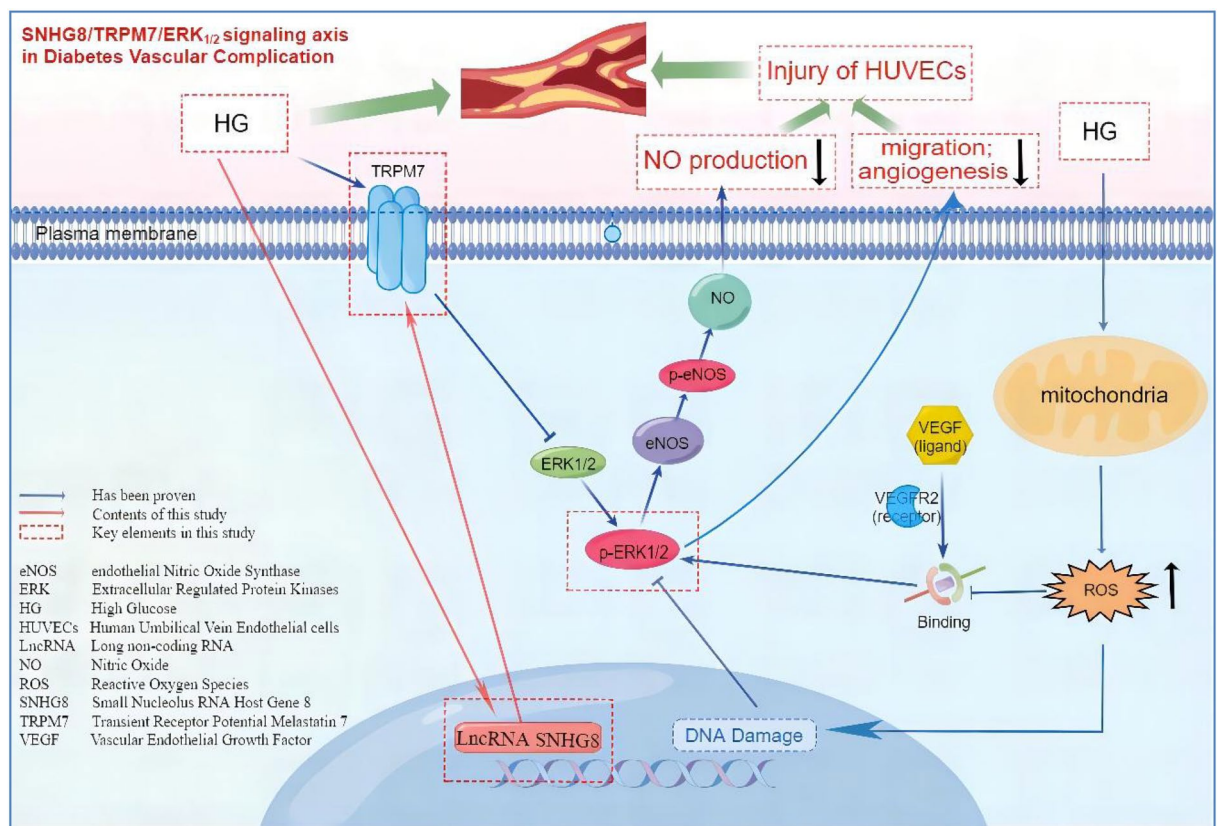


**Figure 7.** Schematic diagram representing the lncRNA SNHG8 plays an important role in HG-induced endothelial cell injury and may regulate the NO production, migration, and angiogenesis of pHUVECs via the TRPM7/ERK<sub>1/2</sub> signaling axis.

## Data availability

All the datasets generated and analyzed in the present study are available from the corresponding author on reasonable request.

Received: 3 March 2023; Accepted: 12 December 2023

Published online: 18 December 2023

## References

- Standl, E. *et al.* The global epidemics of diabetes in the 21st century: Current situation and perspectives. *Eur. J. Prev. Cardiol.* **26**(2), 7–14. <https://doi.org/10.1177/2047487319881021> (2019).
- Beckman, J. A. & Creager, M. A. Vascular complications of diabetes. *Circ. Res.* **118**(11), 1771–1785. <https://doi.org/10.1161/CIRCRESAHA.115.306884> (2016).
- Paneni, F. *et al.* Diabetes and vascular disease: Pathophysiology, clinical consequences, and medical therapy: Part I. *Eur. Heart J.* **34**(31), 2436–2443. <https://doi.org/10.1093/eurheartj/eh149> (2013).
- Chen, X. *et al.* High-density lipoproteins attenuate high glucose-impaired endothelial cell signaling and functions: Potential implications for improved vascular repair in diabetes. *Cardiovasc. Diabetol.* **16**(1), 121. <https://doi.org/10.1186/s12933-017-0605-8> (2017).
- Muñoz-Espín, D. & Serrano, M. Cellular senescence: From physiology to pathology. *Nat. Rev. Mol. Cell Biol.* **15**(7), 482–496. <https://doi.org/10.1038/nrm3823> (2014).
- Mutlak, M. & Kehat, I. Extracellular signal-regulated kinases 1/2 as regulators of cardiac hypertrophy. *Front. Pharmacol.* **6**, 149. <https://doi.org/10.3389/fphar.2015.00149> (2015).
- Molinari, C. *et al.* 1 $\alpha$ ,25-dihydroxycholecalciferol induces nitric oxide production in cultured endothelial cells. *Cell Physiol. Biochem.* **27**(6), 661–668. <https://doi.org/10.1159/000330075> (2011).
- Zhang, Q. *et al.* Endoglin deficiency impairs VEGFR2 but not FGFR1 or TIE2 activation and alters VEGF-mediated cellular responses in human primary endothelial cells. *Transl. Res.* **235**, 129–143. <https://doi.org/10.1016/j.trsl.2021.04.005> (2021).
- Baldoli, E., Castiglioni, S. & Maier, J. A. Regulation and function of TRPM7 in human endothelial cells: TRPM7 as a potential novel regulator of endothelial function. *PLoS One* **8**(3), e59891. <https://doi.org/10.1371/journal.pone.0059891> (2013).
- Zeng, Z. *et al.* TRPM7 regulates vascular endothelial cell adhesion and tube formation. *Am. J. Physiol. Cell Physiol.* **308**(4), C308–C318. <https://doi.org/10.1152/ajpcell.00275.2013> (2015).
- Inoue, K. & Xiong, Z. G. Silencing TRPM7 promotes growth/proliferation and nitric oxide production of vascular endothelial cells via the ERK pathway. *Cardiovasc. Res.* **83**(3), 547–557. <https://doi.org/10.1093/cvr/cvp153> (2009).
- Huang, Y. *et al.* TRPM7 channels play a role in high glucose-induced endoplasmic reticulum stress and neuronal cell apoptosis. *J. Biol. Chem.* **293**(37), 14393–14406. <https://doi.org/10.1074/jbc.RA117.001032> (2018).
- Losko, M., Kotlinowski, J. & Jura, J. Long noncoding RNAs in metabolic syndrome related disorders. *Mediators Inflamm.* **2016**, 5365209. <https://doi.org/10.1155/2016/5365209> (2016).
- Yang, S. N. *et al.* Downregulation of lncRNA SNHG16 inhibits vascular smooth muscle cell proliferation and migration in cerebral atherosclerosis by targeting the miR-30c-5p/SDC2 axis. *Heart Vessels* <https://doi.org/10.1007/s00380-022-02049-4> (2022).
- Chen, B. Z. *et al.* Expression of long non-coding RNA SNHG8 in Epstein-Barr virus-related gastric cancer and clinical outcome. *Zhonghua Bing Li Xue Za Zhi* **46**(2), 84–87. <https://doi.org/10.3760/cma.j.issn.0529-5807.2017.02.004> (2017) (Chinese).
- Huang, T. *et al.* SNHG8 is identified as a key regulator of Epstein-Barr virus (EBV)-associated gastric cancer by an integrative analysis of lncRNA and mRNA expression. *Oncotarget.* **7**(49), 80990–81002. <https://doi.org/10.18632/oncotarget.13167> (2016).
- Ou, K. *et al.* Targeted demethylation at the CDKN1C/p57 locus induces human  $\beta$  cell replication. *J. Clin. Invest.* **129**(1), 209–214. <https://doi.org/10.1172/JCI99170> (2019).
- Schimmack, S. *et al.* A mechanistic role for the chromatin modulator, NAP1L1, in pancreatic neuroendocrine neoplasm proliferation and metastases. *Epigenet. Chromatin.* **7**, 15. <https://doi.org/10.1186/1756-8935-7-15> (2014).
- Lin, Y. *et al.* The fasting blood glucose and long non-coding RNA SNHG8 predict poor prognosis in patients with gastric carcinoma after radical gastrectomy. *Aging Albany NY* **10**(10), 2646–2656. <https://doi.org/10.18632/aging.101576> (2018).
- Bruno, B. *et al.* A protocol for isolation and culture of human umbilical vein endothelial cells. *Nat. Protoc.* **2**, 481–485. <https://doi.org/10.1038/nprot.2007.54> (2007).
- Luo, T. *et al.* Histamine H2 receptor activation exacerbates myocardial ischemia/reperfusion injury by disturbing mitochondrial and endothelial function. *Basic Res. Cardiol.* **108**, 342. <https://doi.org/10.1007/s00395-013-0342-4> (2013).
- Livak, K. J. & Schmittgen, T. D. Analysis of relative gene expression data using real-time quantitative PCR and the 2<sup>(-Delta Delta C(T))</sup> method. *Methods.* **25**, 402–408. <https://doi.org/10.1006/meth.2001.1262> (2001).
- Kurien, B. T. & Scofield, R. H. Western blotting: An introduction. *Methods Mol. Biol. Clifton NJ* **1312**, 17–30. [https://doi.org/10.1007/978-1-4939-2694-7\\_5](https://doi.org/10.1007/978-1-4939-2694-7_5) (2015).
- Liu, X. *et al.* Exploring the role of orexin B-sirtuin 1-HIF-1 $\alpha$  in diabetes-mellitus induced vascular endothelial dysfunction and associated myocardial injury in rats. *Life Sci.* **254**, 117041. <https://doi.org/10.1016/j.lfs.2019.117041> (2020).
- Alp, N. J. & Channon, K. M. Regulation of endothelial nitric oxide synthase by tetrahydrobiopterin in vascular disease. *Arterioscler. Thromb. Vasc. Biol.* **24**(3), 413–420. <https://doi.org/10.1161/01.ATV.0000110785.96039.f6> (2004).
- Folkman, J. Angiogenesis: An organizing principle for drug discovery?. *Nat. Rev. Drug Discov.* **6**(4), 273–286. <https://doi.org/10.1038/nrd2115> (2007).
- Potente, M. & Carmeliet, P. The link between angiogenesis and endothelial metabolism. *Annu. Rev. Physiol.* **79**, 43–66. <https://doi.org/10.1146/annurev-physiol-021115-105134> (2017).
- Treps, L. *et al.* Manipulating angiogenesis by targeting endothelial metabolism: Hitting the engine rather than the drivers—A new perspective?. *Pharmacol. Rev.* **68**(3), 872–887. <https://doi.org/10.1124/pr.116.012492> (2016).
- Warren, C. M. *et al.* A ligand-independent VEGFR2 signaling pathway limits angiogenic responses in diabetes. *Sci. Signal.* **7**(307), ra1. <https://doi.org/10.1126/scisignal.2004235> (2014).
- Yao, R. W., Wang, Y. & Chen, L. L. Cellular functions of long noncoding RNAs. *Nat. Cell Biol.* **21**(5), 542–551. <https://doi.org/10.1038/s41556-019-0311-8> (2019).
- van Solingen, C., Scalamo, K. R. & Moore, K. J. Long noncoding RNAs in lipid metabolism. *Curr. Opin. Lipidol.* **29**(3), 224–232. <https://doi.org/10.1097/MOL.0000000000000503> (2018).
- Yuan, X., Yan, Y. & Xue, M. Small nucleolar RNA host gene 8: A rising star in the targets for cancer therapy. *Biomed. Pharmacother.* **139**, 111622. <https://doi.org/10.1016/j.biopha.2021.111622> (2021).
- Xu, X. *et al.* lncRNA SNHG8 serves as an oncogene in breast cancer through miR-634/ZBTB20 axis. *Cancer Manag. Res.* **13**, 3017–3028. <https://doi.org/10.2147/CMAR.S270128> (2021).
- Yu, B. *et al.* lncRNA SNHG8 promotes proliferation and inhibits apoptosis of diffuse large B-cell lymphoma via sponging miR-335-5p. *Front. Oncol.* **11**, 650287. <https://doi.org/10.3389/fonc.2021.650287> (2021).

35. Tian, J. *et al.* LncRNA Snhg8 attenuates microglial inflammation response and blood-brain barrier damage in ischemic stroke through regulating miR-425-5p mediated SIRT1/NF- $\kappa$ B signaling. *J. Biochem. Mol. Toxicol.* **35**(5), e22724. <https://doi.org/10.1002/jbt.22724> (2021).
36. Zhang, Y. & Bian, Y. Long non-coding RNA SNHG8 plays a key role in myocardial infarction through affecting hypoxia-induced cardiomyocyte injury. *Med. Sci. Monit.* **26**, e924016. <https://doi.org/10.12659/MSM.924016> (2020).
37. Gurney, A. M. Going with the flow: Smooth muscle TRPM7 channels and the vascular response to blood flow. *Circ. Res.* **98**(2), 163–164. <https://doi.org/10.1161/01.RES.0000204554.19924.4a> (2006).
38. Sun, H. *et al.* Role of TRPM7 channels in hyperglycemia-mediated injury of vascular endothelial cells. *PLoS One* **8**(11), e79540. <https://doi.org/10.1371/journal.pone.0079540> (2013).
39. Negri, S. *et al.* Endothelial transient receptor potential channels and vascular remodeling: Extracellular Ca<sup>2+</sup> entry for angiogenesis. *Arterioscler. Thromb. Vasc. Biol.* **40**, 1618. <https://doi.org/10.1161/ATV.00000000000001618> (2020).
40. Khajavi, N. *et al.* TRPM7 kinase is required for insulin production and compensatory islet responses during obesity. *JCI Insight* **8**(3), e163397. <https://doi.org/10.1172/jci.insight.163397> (2023).
41. Zhou, D. M. *et al.* MiR-9 promotes angiogenesis of endothelial progenitor cell to facilitate thrombi recanalization via targeting TRPM7 through PI3K/Akt/autophagy pathway. *J. Cell Mol. Med.* **24**(8), 4624–4632. <https://doi.org/10.1111/jcmm.15124> (2020).
42. Shuang, E. *et al.* 1-Deoxynojirimycin attenuates high glucose-accelerated senescence in human umbilical vein endothelial cells. *Exp. Gerontol.* **55**, 63–69. <https://doi.org/10.1016/j.exger.2014.03.025> (2014).
43. Liang, H. Y. *et al.* Immunomodulatory functions of TRPM7 and its implications in autoimmune diseases. *Immunology* **165**(1), 3–21. <https://doi.org/10.1111/imm.13420> (2022).
44. Scisciola, L. *et al.* Targeting high glucose-induced epigenetic modifications at cardiac level: The role of SGLT2 and SGLT2 inhibitors. *Cardiovasc. Diabetol.* **22**(1), 24. <https://doi.org/10.1186/s12933-023-01754-2> (2023).
45. Roskoski Jr, R. A historical overview of protein kinases and their targeted small molecule inhibitors. *Pharmacol. Res.* **100**, 1–23. <https://doi.org/10.1016/j.phrs.2015.07.010> (2015).
46. Liu, T. *et al.* Attenuation of exogenous angiotensin II stress-induced damage and apoptosis in human vascular endothelial cells via microRNA-155 expression. *Int. J. Mol. Med.* **31**(1), 188–196. <https://doi.org/10.3892/ijmm.2012.1182> (2013).

## Acknowledgements

We sincerely thank all the staff in the Department of Central laboratory, the first affiliated Hospital of Fujian Medical University for their help in this study.

## Author contributions

F.P. and Y.L. initiated and designed the study. J.L. and F.P. supervised the study. Material preparation, data collection and analysis were performed by Z.F., J.Y., S.Z. and C.X. The first draft of the manuscript was written by Z.F., X.C. and L.W. All authors read and approved the final manuscript. All authors consent to publication.

## Funding

This study was supported by Foreign Cooperation Project of Science and Technology, Fujian Province (No.202110013); Joint Funds for the innovation of science and Technology, Fujian province (No. 2021Y9121); Fujian provincial health technology project (No. 2020QNA056); Natural Science Foundation of Fujian Province (No. 2022J01686); The scientific research personal training project for the Fujian Provincial Health Commission (NO.2019-1-40); Scientific Research Project of Hefei Third People's Hospital (No. SYKZ202201).

## Competing interests

The authors declare no competing interests.

## Additional information

**Supplementary Information** The online version contains supplementary material available at <https://doi.org/10.1038/s41598-023-49779-7>.

**Correspondence** and requests for materials should be addressed to Y.L. or F.P.

**Reprints and permissions information** is available at [www.nature.com/reprints](http://www.nature.com/reprints).

**Publisher's note** Springer Nature remains neutral with regard to jurisdictional claims in published maps and institutional affiliations.



**Open Access** This article is licensed under a Creative Commons Attribution 4.0 International License, which permits use, sharing, adaptation, distribution and reproduction in any medium or format, as long as you give appropriate credit to the original author(s) and the source, provide a link to the Creative Commons licence, and indicate if changes were made. The images or other third party material in this article are included in the article's Creative Commons licence, unless indicated otherwise in a credit line to the material. If material is not included in the article's Creative Commons licence and your intended use is not permitted by statutory regulation or exceeds the permitted use, you will need to obtain permission directly from the copyright holder. To view a copy of this licence, visit <http://creativecommons.org/licenses/by/4.0/>.

© The Author(s) 2023